The DEIMOS flexure compensation system: overview and operational results

Robert I. Kibrick[a], Steven L. Allen[a], De A. Clarke[a], Sandra M. Faber[a], Andrew C. Phillips[a], and Gregory D. Wirth[b]

[a]UCO/Lick Observatory
University of California
Santa Cruz, California 95064 USA

[b]W. M. Keck Observatory
Kamuela, Hawaii 96743 USA

ABSTRACT

The DEep Imaging Multi-Object Spectrograph (DEIMOS) was commissioned on Keck II in June 2002.[1] It employs a closed-loop flexure compensation system (FCS) to measure and compensate for image motion resulting from gravitationally-induced flexure of spectrograph elements.[2] The FCS utilizes a set of fiber-fed FCS light sources located at the edges of the instrument focal plane to produce a corresponding set of spots on a pair of FCS CCD detectors located on either side of the science CCD mosaic. (This FCS light follows the same light path through the instrument as the science spectra.) During science exposures, the FCS detectors are read out several times per minute. These FCS images are analyzed in real time to measure any translational motion of the FCS spots and to derive correction signals; those signals drive active optical mechanisms which steer the spots back to their nominal positions, thus stabilizing the images on the FCS CCDs and the science mosaic.

This paper describes the commissioning of the DEIMOS FCS system, its continued evolution during its first 18 months of operation on the telescope, and its operational performance over that period. We describe the various challenges encountered while refining the initial FCS prototype (deployed at commissioning) into a fully-operational and highly-reliable system that is now an essential component of the instrument. These challenges include: reducing stray light from FCS light sources to an acceptable level; resolving interactions between FCS acquisition and slit mask alignment; providing robust rejection of cosmic ray events in FCS images; implementing a graphical user interface for FCS control and status.

Keywords: spectrograph active flexure compensation, stray light, DEIMOS

1. INTRODUCTION

DEIMOS is a general purpose, faint-object, multi-slit spectrograph whose key features are wide spectral coverage, high spectral resolution, high throughput, and long slit length on the sky. The instrument is housed in a cylindrical enclosure which rotates[3] to counteract the field rotation inherent in an alt-az telescope. DEIMOS requires an active FCS, because without one, flexure induced image motion exceeds 20 pixels over a 360° rotation (see Sect. 5), or several pixels over a typical hour-long set of slitmask observations. The magnitude of this flexure depends on the operational mode.

DEIMOS operates in three modes: direct imaging, single-object spectroscopy, and multi-object spectroscopy. For spectroscopy, a remotely-operable slit mask mechanism enables rapid insertion of and switching between a single longslit mask and up to ten multi-slit masks, while for direct imaging the mechanism retracts all masks from the optical path.

Further author information- (Send correspondence to R.K)
R.K.: Email: kibrick@ucolick.org; http://www.ucolick.org/~kibrick; Telephone: 831-459-2262; Fax: 831-459-2298;
S.A.: Email: sla@ucolick.org; Telephone: 831-459-3046; D.C.: Email: de@ucolick.org; Telephone: 831-459-2630;
S.F.: Email: faber@ucolick.org; Telephone: 831-459-2944; D.P.: Email: phillips@ucolick.org; Telephone: 831-459-2476;
G.W.: Email: wirth@keck.hawaii.edu; Telephone: 808-881-3866

DEIMOS offers a choice of gratings and grating tilts via three movable mechanisms, called sliders. One slider holds the mirror used for direct imaging and the other two hold the gratings used for spectroscopy; the former operates at a fixed tilt while each of the latter includes a precision grating tilt mechanism capable of tilting a grating through an angle of nearly 40 degrees. Each of the two grating sliders can accept several different grating cells, but removal and insertion of grating cells is a manual process performed during the daytime. A remotely-controlled mechanism enables astronomers to switch between the different sliders during observing. The time required to change between sliders varies between 2 and 4 minutes.

As shown in Fig. 1, DEIMOS utilizes a set of fiber-fed FCS light sources mounted to the ends of the slitmask form to produce a corresponding set of spots on a pair of FCS CCD detectors located on either side of the science CCD mosaic. Not shown in Fig. 1 are the science filter wheel and the shutter, both of which are located between the camera and the mosaic focal plane. That shutter must be open for light to reach either the FCS or the mosaic CCDs. During science exposures, the FCS detectors are read out several times per minute to measure any motion of the FCS spot images. Correction signals are derived from those measurements and used to drive active optical mechanisms which steer the spots back to their nominal positions. By stabilizing the FCS spot images on the FCS CCDs, the science spectra are stabilized on the science mosaic (see Fig. 2).

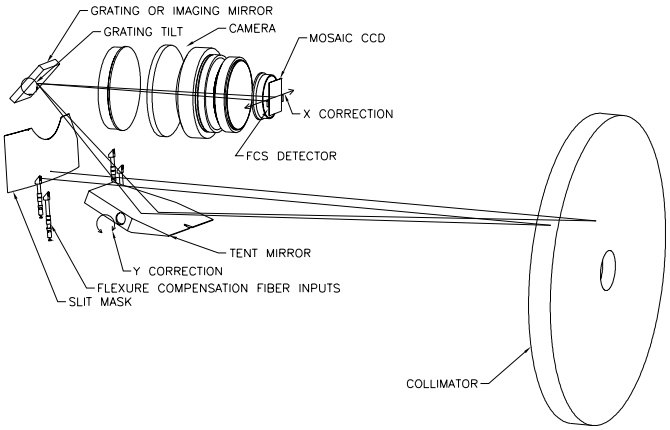

Figure 1. Simplified optical overview of DEIMOS FCS

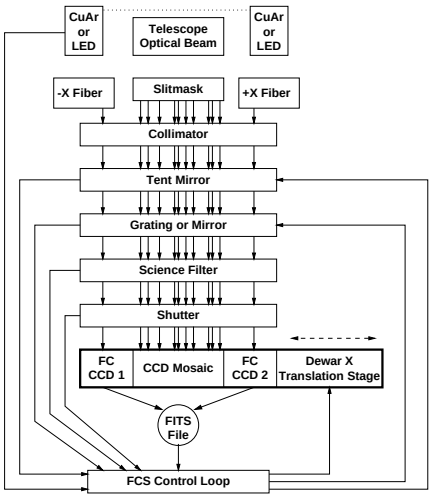

Figure 2. Block diagram of DEIMOS FCS

The DEIMOS FCS is designed to maintain constant image position on the detector over short time scales as the spectrograph rotates, and over longer time scales between the afternoon flat-field calibrations and evening observing. As position angle changes, flexural deformation of the optical supports causes image motion on the detector, while additional image motion is caused by imperfect re-positioning of the optical elements. Most important are the gratings, which frequently move as sliders are repositioned during an observing run or whenever the grating complement is manually altered prior to a run.

DEIMOS compensates for these short and long time scale motions via a tiltable tent mirror, which steers the image in the DEIMOS Y coordinate (along the spectrum), and a translation stage within the dewar, which moves the position of the science CCD mosaic in the DEIMOS X coordinate (along the slit). In addition, when operating in spectroscopic mode, the image can also be steered in Y using the grating tilt mechanism of the selected slider; this is necessary whenever the image motion in that axis demands a correction that exceeds the operating range of the tent mirror. This extra compensation range in Y is not available (nor is it needed) in direct imaging mode (see Sect. 2.2), since the slider that holds the imaging flat mirror holds it at a fixed tilt.

The DEIMOS FCS can only compensate for image translation errors and cannot compensate for image motion due to rotation or changes in image scale. However, it is able to compensate for errors that result from other sources, such as temperature change across the instrument, mechanical hysteresis in moving mechanisms or in camera cell supports, or zero point shifts due to slider re-positioning errors or grating cell re-insertion errors. In addition, because DEIMOS has FCS CCDs located on either side of the science CCD mosaic, it can measure and report both image rotation and changes in image scale even if it cannot correct for them.

2. HARDWARE COMPONENTS

2.1. FCS fibers and light sources

The FCS fibers and light sources are used to generate a set of artificial objects in the focal plane. A set of optics at the telescope focal-plane-end of each fiber produces an output cone at f/15 so as to match the f/ratio of the output beam from the telescope. Four 200 micron core fibers are used, with two fibers mounted to the $-X$ edge of the slitmask and the other two to the $+X$ edge (see Fig. 3). The pair of fibers on each edge are nearly centered along the Y axis but are slightly offset from one another in Y (the dispersion axis) so that the spectra they generate are offset in wavelength. This helps ensure the availability of usable spectral features in the FCS spectra.

The far end of each fiber is illuminated by one of two remotely controlled light sources: a CuAr arc lamp or a white light LED (all four fibers are illuminated with the same light). The CuAr lamp produces a rich spectrum with broad wavelength coverage (see Fig. 4), and can be used in either spectroscopic or direct-imaging modes. The LED can be used whenever the currently-selected science filter renders the CuAr lamp too bright for use in direct imaging mode. (The light emitted from the ends of the FCS fibers travels through all the same optical elements as the light that passes through the slits in the slitmask, so the intensity of FCS light that reaches the FCS CCDs depends on the transmission characteristics of the currently selected filter and grating.)

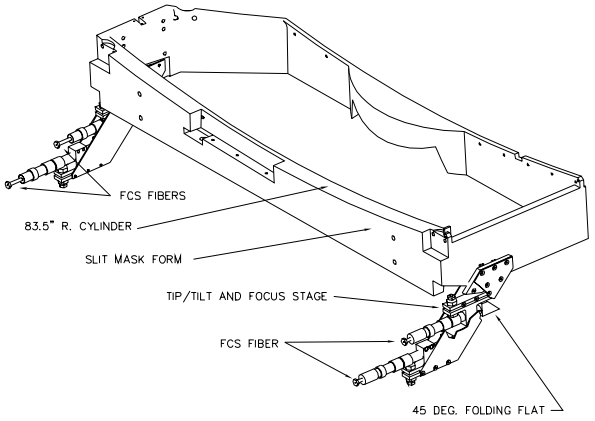

Figure 3. FCS fiber attachments to slitmask form

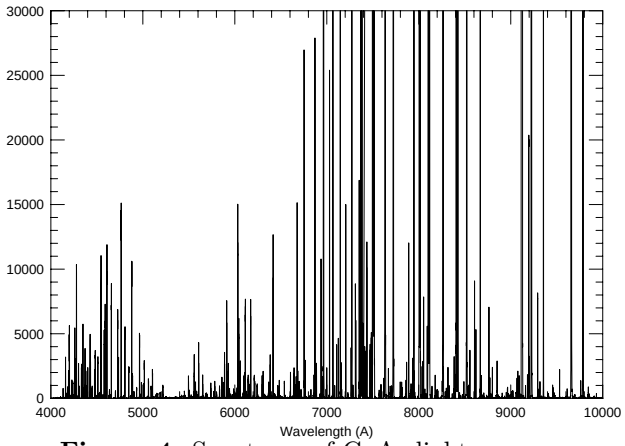

Figure 4. Spectrum of CuAr light source

2.2. Tent mirror

The tent mirror receives the output beam from the collimator and reflects it onto either a grating or the direct imaging mirror (see Fig. 1). The tent mirror pivots in one axis and is used to steer the image in DEIMOS Y (spectral direction). We decided to use the tent mirror for this task, instead of using a separate Y-translation stage in the dewar, because it was mechanically simpler. Due to anamorphic magnification in the spectrograph, the range over which the tent mirror can steer the image varies by a factor of 1.8 depending on the grating tilt. The maximum range is 23.2 pixels when using the mirror for direct imaging and the minimum is 12.9 pixels when using the 1200-groove/mm grating at its reddest tilt. Unfortunately, for some gratings and tilt ranges, the image steering range of the tent mirror is insufficient to compensate fully for the observed image motion in the DEIMOS Y axis. In those cases, additional range is provided by using the grating tilt mechanisms.

2.3. Grating tilt mechanisms

Each of the two grating sliders contains a tilt mechanism with a range of nearly 40°. Each mechanism is driven by a servo motor via a multi-stage friction drive that provides nearly backlash-free positioning. A Gurley incremental encoder is directly coupled on-axis to the tilt axis of each mechanism via an anti-torque arm mechanism and provides a tilt angle resolution of 1.44 arc-seconds per encoder count. This translates to an average image-steering resolution of 0.3 pixel on the detector.

2.4. Dewar translation stage

A translation stage within the dewar moves the position of the science CCD mosaic (and the attached FCS CCDs) in the DEIMOS X coordinate, i.e., perpendicular to the dispersion (see Fig. 5). This stage provides an image steering range of 26.4 pixels with an effective resolution of 0.01 pixel.

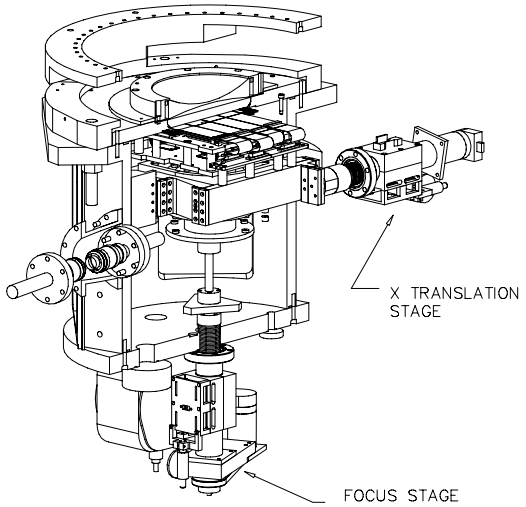

Figure 5. Dewar translation stage

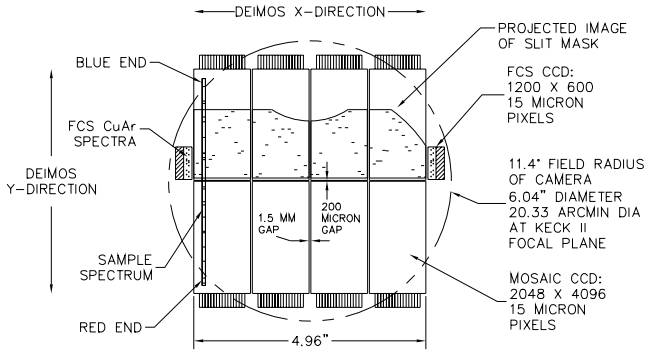

Figure 6. FCS CCDs and science CCD mosaic

2.5. FCS CCDs and controller electronics

A 600 row by 1200 column FCS CCD is mounted on each side ($-X$ and $+X$) of the DEIMOS mosaic (see Fig. 6). These devices are unthinned, front-side illuminated, and have 15 micron pixels (the same pixel size as on the science mosaic CCDs). They are mounted parfocal with the science CCD mosaic and are rigidly mounted to the same backplane so as to minimize any flexure of the FCS CCDs relative to the science CCD mosaic.

The FCS CCD controller electronics are implemented using the same type of San Diego State University (SDSU) second generation controller boards[4] as are used for the science mosaic CCD controller.[5] However, the FCS CCD controller and the science mosaic controller use completely independent hardware and software, and each subsystem can be run autonomously. Electronic cross-talk between these two separate systems (whose CCDs are co-resident in the same dewar) is not an issue since the times at which they read out are mutually exclusive: the FCS CCDs are read out only during the course of an exposure when the shutter is open, while the science mosaic CCDs are read out only at the end of the exposure when the shutter is closed. Thus, there was no need to synchronize the clocks of these two subsystems.

3. EVOLUTION OF THE FCS CONTROL SOFTWARE

The objective of the FCS system is to measure changes in the positions of spectral features (or FCS fiber images if in direct imaging mode) imaged by the FCS CCDs in order to generate an error signal resulting in updated settings for the FCS mechanisms (i.e., the tent mirror and dewar translation stage). The updated settings for those mechanisms are intended to steer the positions of those features back to their nominal values so as to stabilize the images on the FCS CCD and the science mosaic.

Because the uncontrolled flexure-induced image motion in DEIMOS is nearly as large as the compensation range of the FCS tent mirror and dewar translation mechanisms, the nominal positions for those features should be measured only when: (1) those mechanisms have been driven to the center of their respective ranges of travel, and (2) any grating tilt offsets are set to zero, *and* (3) the instrument is rotated to a position angle that corresponds to the center of the flexure range for the currently selected slider. Otherwise, if the nominal positions of those features are measured at an arbitrary instrument position angle or with the FCS mechanisms not properly nulled, the FCS control loop might ultimately fail to stabilize those images because it has driven one of those mechanisms to its limit of travel.

3.1. Prototype software implementation

The prototype implementation of the DEIMOS FCS software, deployed during instrument commissioning in July 2002, tracked the position of a single, selected feature* on one of the two FCS CCDs.[2] That implementation supported several basic functions that were initially written as scripts:

fcszero rotates DEIMOS to the instrument position angle that corresponds to the center of the DEIMOS Y flexure curve for the currently selected slider and drives the FCS mechanisms (tent mirror and dewar translation stage) to their respective range-of-travel centers;

fcsref enables the observer to select and record the reference position of the FCS feature that will be used as the reference spot for the current instrument configuration;

fcstrack enables the FCS control loop so that it will try to hold the reference spot at the reference position whenever the shutter remains open for a sufficient period of time to allow an FCS image to be acquired.

During the afternoon, the observer acquires science-mosaic arc-lamp and flat-field exposures for each of the instrument configurations planned for that night's observing. For each configuration that involves a distinct combination of grating, grating tilt, and filter, the observer first performs the *fcszero* and *fcsref* functions, and then proceeds (with the instrument parked at the position angle set by the *fcszero* function) to take the calibration images for that configuration. *Fcstrack* is enabled during those calibrations to correct for any thermally-induced image motion.

During the night, the observer enables the *fcstrack* function, which monitors the current instrument configuration. Whenever *fcstrack* detects a configuration change involving a filter, a grating, or a grating tilt, it attempts to acquire the reference spot that was identified for that particular configuration during the afternoon calibrations. *Fcstrack* adjusts the FCS mechanisms on each iteration (typically twice per minute) so that that reference spot is held at its reference position. (If no reference spot is defined for a given configuration, then the FCS becomes idle until another configuration having a defined reference spot is selected.) Thus, science exposures acquired during the night are maintained in registration with calibration exposures taken during the afternoon.

3.2. Updated FCS software implementation

In early 2003, the FCS algorithm was updated to its present form. FCS image motion is now measured by cross-correlating each new FCS spectrum with its corresponding reference spectrum that was obtained during afternoon calibrations. Since two fibers are used to illuminate each of the two FCS CCDs, four FCS spectra are generated on each cycle of the FCS control loop. (If DEIMOS is being operated in direct imaging mode, then there are two FCS fiber images on each of the two FCS CCDs.) Both FCS CCDs are read out together and written to a common FITS image file.

In the updated version of the FCS software, while the *fcszero* function remains unchanged, the *fcsref* and *fcstrack* functions have been revised. *Fcsref* now saves the FITS image file that contains the FCS reference spectra (or FCS fiber images) from each of the two FCS CCDs; it also tags this FITS file so that it is identified as the FCS reference image file that corresponds to the configuration of the instrument at which those reference spectra (or fiber images) were obtained. *Fcstrack* now performs cross-correlations of the current FCS spectra (or fiber images) with their corresponding FCS reference spectra (or reference fiber images) contained within the FCS reference image file that was recorded by *fcsref* during the afternoon calibrations.

3.3. Graphical user interfaces for FCS control and status

A key element of converting the DEIMOS FCS software from an experimental prototype to a fully-operational turnkey system was development of a graphical user interface (GUI) for control of FCS functions and display of FCS status.† The features provided by this GUI greatly simplify the task of acquiring FCS reference images during the afternoon as well as monitoring the automatic operation of FCS during nighttime observing.

*That feature is referred to as the FCS *reference spot*; the FCS CCD pixel coordinates at which the FCS tries to hold that reference spot are denoted as the *reference position*.

†The DEIMOS FCS GUI was developed using the *dashboard* software[6] that is common to the GUIs for several Keck optical instruments: ESI, DEIMOS, and the HIRES exposure meter.

The top-level panel of the FCS GUI is shown in Fig. 7. It provides a compact and color-coded display of the current state of the FCS system, along with buttons for calling up sub-panels that provide additional levels of detail. For example, clicking on the **Setup** button brings up a sub-panel which contains buttons for invoking the functions (e.g., *fcszero* and *fcsref*) used to acquire the FCS reference images during the afternoon calibrations for each configuration of the instrument. During nighttime observing, observers can use other buttons on the top-level panel to invoke additional sub-panels to monitor FCS tracking performance and to identify conditions that may interfere with FCS operation.

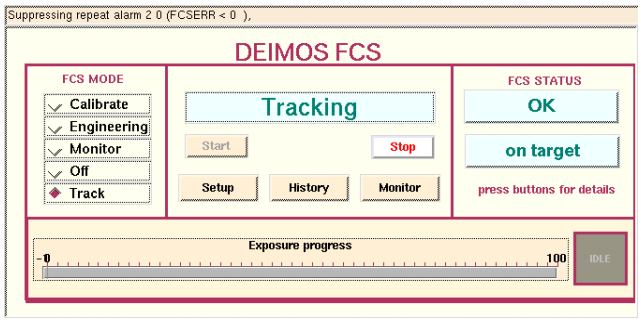

Figure 7. FCS dashboard

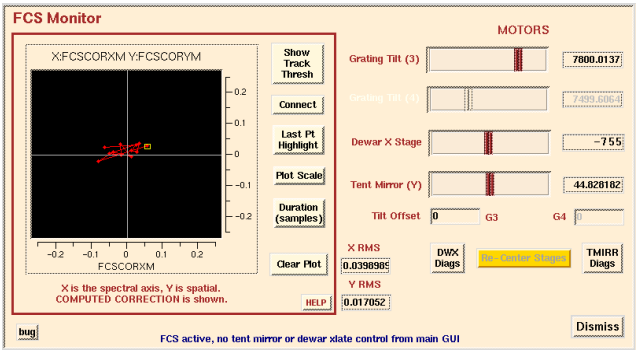

Figure 8. FCS monitor panel

The FCS monitor panel (shown in Fig. 8) provides a running X-Y scatter plot of the FCS residual tracking errors measured over the course of the current science exposure, along with a display of the current RMS FCS tracking error. This panel also provides a display of the positions of the relevant FCS beam-steering mechanisms with respect to the total range of travel for each such mechanism. The FCS tracking panel (shown in Fig. 10) provides time-scrolled plots of the various FCS tracking errors individually measured by the two FCS CCDs, along with a display of the number of FCS images that were rejected (e.g., due to cosmic ray events) during the current exposure of the science mosaic.

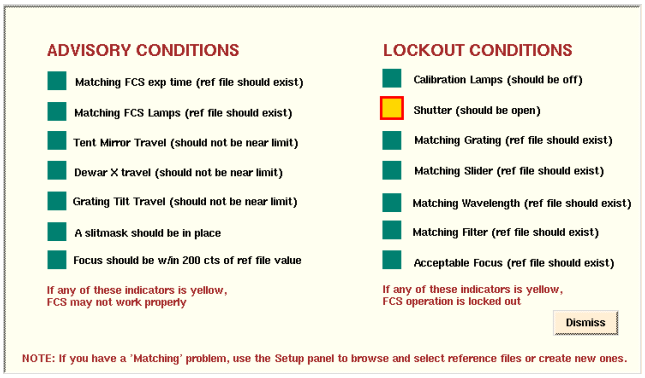

Figure 9. FCS lockout panel

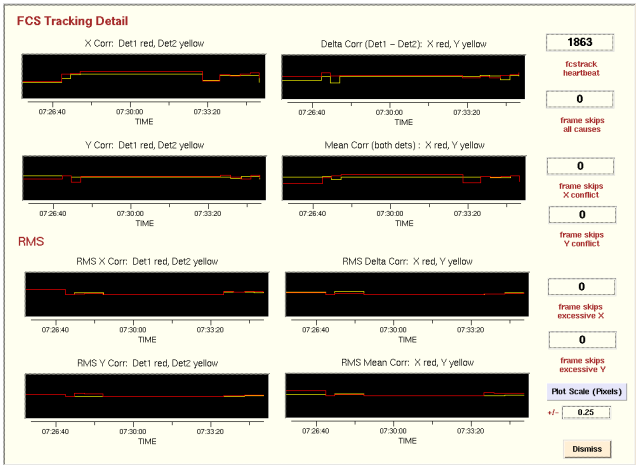

Figure 10. FCS tracking panel

The FCS advisory and lockout panel (shown in Fig. 9) provides a set of indicator lamps that turn yellow to indicate a condition that may interfere with FCS operation or that will lock out its operation entirely. In this example, FCS operation is locked out because the shutter is closed, thus preventing the FCS CCDs from receiving the light from the FCS fiber sources. In the case of more serious problems, the FCS GUI will also generate pop-up alarm boxes in the foreground to ensure that such problems are not overlooked by the observer.

4. OPERATIONAL CHALLENGES

In the course of refining the initial FCS prototype software into a fully-operational turnkey system, several significant operational challenges were identified. Based on the operational experience obtained during instrument commissioning and early shared-risk science observing, solutions to these challenges were identified and successfully implemented.

4.1. Arbitration of the main shutter

The FCS CCDs and the science mosaic CCDs reside in the same dewar and share a common shutter. That shutter is controlled by the science mosaic CCD controller, which routinely keeps that shutter closed unless the science mosaic CCDs are being used to take a non-dark exposure. However, whenever that shutter is closed, light from the FCS fiber-fed sources cannot reach the FCS CCDs, and, as a result, the FCS can neither measure nor correct for flexure-induced image motion.

The temporary disabling of the FCS that occurs whenever the shutter is closed represents a significant operational challenge. For example, whenever the telescope is slewed a large distance to acquire the next target, a large change in parallactic angle typically occurs, resulting in a correspondingly large rotation of the DEIMOS instrument as it tracks the rotation of the telescope field. That large rotation generates, in turn, significant flexure-induced image motion within the instrument.

As long as the shutter remains closed while the telescope is slewed, the resulting image motion remains undetected and uncompensated. When the next science exposure is started and the shutter opens, only then does the FCS discover that it needs to command a large correction to the FCS beam-steering mechanisms. Because at least one complete FCS correction cycle is needed before that correction is fully applied, the first tens of seconds of the science mosaic exposure are integrated on a mis-registered image.

During commissioning, observers had to remember that following a large slew of the telescope, they needed to interactively command the shutter open and wait for the FCS to re-converge prior to starting the next exposure of the science mosaic. This requirement reduced observing efficiency and increased the potential for observer error.

To address this problem, the *fcstrack* software now monitors the overall state of the instrument and automatically commands the shutter open whenever it determines that: 1) the science mosaic CCD system is idle and 2) no calibration lamps are turned on. As a result, during nighttime observing, the shutter now remains open most of the time, as it is typically commanded closed only when the science mosaic CCDs are erasing or reading out. This significantly increases the fraction of time during which the FCS is enabled to make corrections and allows those corrections to continue on a regular basis while the telescope is being slewed (and the instrument rotated) to the next target.

Because the shutter now remains open during much of the time that the telescope is slewing, this solution poses a small risk that the science mosaic CCDs might be overexposed if the instrument were configured for direct imaging and the telescope trajectory to the next target traversed the path of a very bright object like the Moon. In cases where this is a concern, bright light from the sky can be blocked by temporarily closing the hatch at the front of the instrument while the telescope is slewed, while still enabling FCS light to reach the FCS CCDs through the open shutter. Alternatively, the total amount of bright light from the sky able to reach the science mosaic can be reduced by temporarily inserting a slitmask or an appropriate filter.

4.2. Cosmic ray rejection

Like any CCD, the FCS CCDs will occasionally experience image artifacts caused by cosmic rays. When such artifacts are sufficiently intense and/or close to image features in the FCS spectra (or fiber images if in direct imaging mode), those artifacts can skew the image displacement measurements computed by the FCS. If the FCS used such skewed measurements to derive corrections to the settings of the FCS beam-steering mechanisms, that could cause incorrect settings to be applied to those mechanisms and result in the unintended smearing of the science mosaic exposure currently in progress. If those incorrect settings were sufficiently in error, subsequent FCS spectra could become so far out of registration with their corresponding reference spectra that the FCS could lose its servo lock altogether.

To protect against such problems (as well as for several other reasons), the FCS derives a separate set of image displacement measurements from each of the two FCS CCDs. Given that the two FCS CCDs are located on opposite sides of the science mosaic, it is highly unlikely that a single cosmic ray event would impact both CCDs in the same way, or that two separate cosmic rays would produce similar effects on both CCDs during the same FCS CCD integration. Accordingly, a cosmic ray event that significantly perturbs the image displacement measurement derived from one of the two FCS CCDs is unlikely to affect the corresponding measurement from the other CCD, and the two measurements will disagree. In the case of such a disagreement, the current FCS correction cycle could be skipped and a new pair of FCS exposures immediately started.

Unfortunately, implementation of this cosmic ray rejection concept proved more complicated than originally anticipated, because other factors can cause the image displacement measurements derived from the two FCS CCDs to disagree. For example, the passive thermal compensators that adjust the spacing between elements of the DEIMOS camera are not completely effective; as a result, temperature changes in the camera can induce small changes in its image scale. Since the FCS CCDs are located at the edges of the camera's field, changes in camera image scale result in opposite changes in the DEIMOS X coordinate (spatial direction) position of corresponding FCS spectral features on the two FCS CCDs. Similarly, flexure-induced rotations of the DEIMOS image (for which the FCS cannot compensate) result in opposite changes in the DEIMOS Y coordinate (spectral direction) position of corresponding FCS features.

Accordingly, if FCS correction cycles were inhibited whenever there was any significant disagreement between the image displacement measurements separately derived from the two FCS CCDs, most correction cycles would be skipped and the FCS would be ineffective. To discriminate between those disagreements that are a result of image rotation or temperature-induced changes in camera image scale and those disagreements that are the result of cosmic rays, it is important to note that the former occur gradually over relatively long time scales whereas the latter occur abruptly.

This discrimination can be effectively performed by first computing (separately for each FCS CCD) the incremental change in image position (as measured by the current FCS exposure compared to that measured by the immediately previous FCS exposure) and then looking for disagreement in that incremental change as separately measured by the two FCS CCDs. In the case of cosmic ray events that significantly perturb the image displacement measurement from one of the two FCS CCDs, there will be a large disagreement between incremental change in image position measured by each CCD, and that disagreement can be used to signal that the current FCS correction cycle should be skipped.

It is worth noting that in computing the corrections to apply to the FCS beam-steering mechanisms, the FCS uses the average of the image displacement measurements derived from the two FCS CCDs. Thus, to first order, the effects of image rotation and temperature-induced changes in camera image scale are averaged out (because the dominant axis of each of these two effects has opposite sign on each of the two CCDs) and do not alter the corrections generated by the FCS.

4.3. Scattered light from FCS CuAr sources

An important consideration in designing the FCS system is the amount of scattered light from FCS spectra that escapes over onto the science detector. The FCS spectra must be quite bright compared to the science spectra, as good S/N must be obtained in FCS exposure times as short as 10 s or less.

The density of lines must also be high so that lines are available with all dispersions and grating tilts. As we have noted, the latter requirement led to our choice of a CuAr lamp, with its very rich spectrum of lines. However, a drawback of the CuAr spectrum, as shown in Fig. 4, is that the lines in the blue are roughly 30 times dimmer than the brightest lines in the red. If a bare lamp with no color-balancing filter is used, making the blue lines bright enough requires turning the lamp brightness so high that the red lines are tremendously bright, with the result that too much scattered FCS light spills out onto the science detector.

4.3.1. Initial attempts to reduce scattered light

Our first configuration ran the FCS light source at high intensity and with no filter. We estimated that 5% of the light falling onto each FCS detector was scattered onto the portions of the science detector nearest to

it. The scattered light intensity in 1000 s near the FCS detectors was a few hundred photons per pixel, clearly unacceptable.

Prior to commissioning, scattered light was significantly reduced by: (1) turning down the overall light intensity by mis-aiming the collimated CuAr light beam shining on the ends of the fibers, (2) by inserting a color-balancing BG38 filter[‡] to attenuate the red light, and (3) by inserting an opaque baffle between the field flattener and the dewar window to intercept light in the FCS spectra that will fall outside the FCS detectors.

Unfortunately, once all of the light leaks and other sources of stray light inside the instrument were identified and corrected during commissioning, it was determined that the residual scattered light from the FCS spectra was still detectable in images from the science mosaic. While that scattered light could be further reduced by additional reductions in the intensity of the light emitted by the FCS fibers, doing so would require a corresponding increase in FCS exposure times, thus reducing both the frequency of FCS correction cycles and the level of image stabilization that FCS could provide.

4.3.2. Alternative solutions

One suggested solution to this problem proposed manual insertion or removal of a neutral density filter between the CuAr lamps and the entrance end of the FCS fibers; that ND filter would be inserted when observing at redder wavelengths (where the CuAr lines are extremely bright) and removed when observing at bluer wavelengths (where the CuAr lines are faint). However, accessing the portion of the instrument that houses the CuAr lamps requires removal of one of the instrument cladding panels, and these panels were not designed for frequent removal and re-attachment. In addition, while this operation could be done during the afternoon, it is not practical to do at night. Thus, while this solution might have been feasible for some observing programs that operate at a limited range of wavelengths, it would not have been feasible for those programs that observe both in the blue and in the red during the same night.

A variation of this solution would be to install a remotely-operable filter wheel (loaded with ND filters of varying opacity) between the CuAr lamps and the fiber inputs. However, there is insufficient space to add such a mechanism and such an addition would significantly increase the complexity and cost of the FCS system.

4.3.3. Shuttering of the FCS CuAr light at its source

A simpler and less costly solution is obtained by shuttering (or otherwise interrupting) the CuAr light so that it only enters the FCS fibers during the time that the FCS CCDs are integrating. Doing so reduces the amount of FCS scattered light that the science mosaic detects, because the FCS CCDs are integrating for only a fraction of each FCS correction cycle. There is no point in sending CuAr light down the FCS fibers during the period of time when the FCS CCDs are erasing or reading out, nor during the time the FCS images are being analyzed or the settings of the FCS mechanisms updated. By shuttering the CuAr light so that it only enters the FCS fibers when the FCS CCDs are integrating, the amount of FCS scattered light that spills onto the science mosaic can be reduced by a factor of 10 to 20, depending upon the FCS CCD exposure time.[§] Such an approach reduces the scattered light to a level where it is no longer detectable on the science mosaic in integrations of 1200 s, even when operating at redder wavelengths where the CuAr lamps are bright.

As mentioned in Sect. 2.5, the science mosaic CCDs and the FCS CCDs are each operated by their own independent CCD controller. Each controller provides its own shutter control signal. That signal from the science mosaic controller is used to operate the large, dual-bladed shutter located directly in front of the dewar window. The shutter control signal from the FCS CCD controller was originally unused, but was readily available for shuttering the light from the CuAr lamps.

The shuttering of the CuAr light could be accomplished either with an electro-mechanical shutter or by pulsing the power to the CuAr lamp. In the hope of avoiding the cost, mechanical complexity, and reliability

[‡]See $http://www.us.schott.com/optics\_devices/english/download/index.html?ND=1\&DOWNLOADFILE2=/optics\_devices/english/download/bg-38.pdf\&BAUID=372160$

[§]An additional benefit to shuttering the light from the CuAr lamp is that the CuAr spectral features imaged on the FCS CCDs no longer exhibit faint vertical trails. Previously, when the CuAr lamp was left on continuously during FCS operation, such faint vertical trails in the FCS images resulted from CuAr light that illuminated the FCS CCDs during their respective erase and readout cycles.

issues associated with adding an electro-mechanical shutter, we decided to first try pulsing the power to the CuAr lamp. This was accomplished simply by adding a solid-state relay in series with the power to the CuAr lamp, and using the shutter control signal from the FCS CCD controller to activate that relay. What was not known at the time was whether pulsing the CuAr lamp on (typically for 1 to 2 seconds) and off again (typically for 20 seconds) hundreds of times per night would result in significantly reduced CuAr lamp lifetimes or in instability in the ratio of the CuAr spectral line strengths.

After operating the DEIMOS FCS system in this mode for 18 months, we have seen no evidence of either problem. Accordingly, we conclude that pulsing the power to the CuAr lamp so that it is only illuminated during the times that the FCS CCDs are integrating provides a simple and cost-effective solution to the problem of residual scattered light from the FCS spectra.

4.4. Interactions between FCS acquisition and slit mask alignment

When using DEIMOS to obtain multi-slit spectra for a given target field, the observer commands a remotely-operated actuator to insert a custom slitmask[7] (specifically designed for that field) onto the slitmask form (see Fig. 3). Then the telescope pointing and the DEIMOS rotator angle are adjusted until the light from each of several relatively bright alignment stars is properly centered in its corresponding alignment box on the slitmask.[¶] This process is known as slitmask alignment.

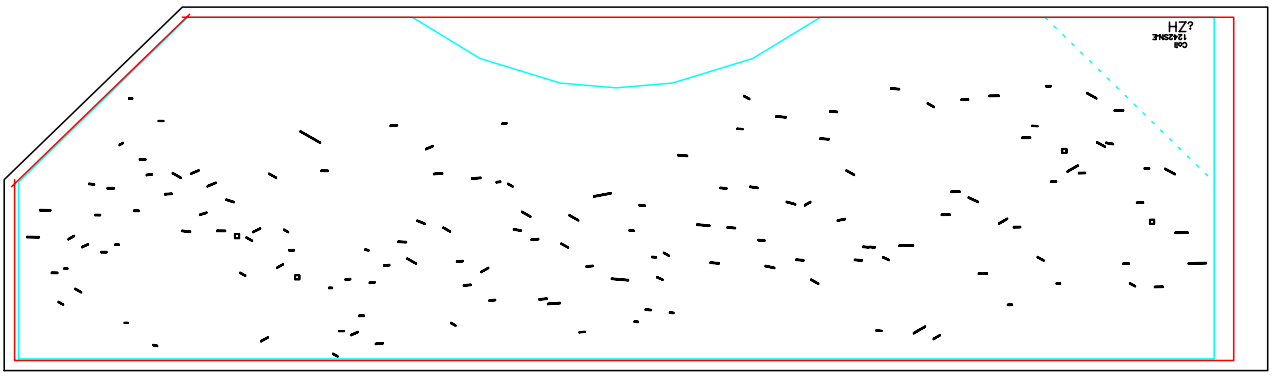

Figure 11. Example DEIMOS slitmask showing alignment holes, vignetted region, and engraved ID

To take these slitmask alignment images, DEIMOS must be temporarily reconfigured from spectroscopic to direct imaging mode. That can be accomplished either by switching from the grating slider to the mirror slider, or by keeping the grating slider in position and tilting the grating so that it operates at 0-order.[‖] In either case, changing the instrument configuration from spectroscopic to direct imaging (and then back again), has implications for the FCS, because such configuration changes alter the pattern of FCS spots that project onto the FCS CCDs.

As noted in Sect. 3.1, if the instrument configuration is changed to one for which a corresponding FCS reference image was not taken during afternoon calibrations, the FCS automatically enters an idle state. But if the current FCS configuration matches one for which a corresponding FCS reference image exists, then FCS automatically starts correcting so as to keep the current FCS spectra aligned with the corresponding FCS reference spectra taken during the afternoon. For example, if FCS reference spectra were obtained for the 0-order configuration during the afternoon, then FCS would attempt to make corrections whenever the instrument was subsequently configured to that matching 0-order setting.

[¶]The alignment boxes are square holes typically $4''$ across that are milled into the slitmask along with the slits for the multi-slit spectra. Slitmasks have a usable length of 73.3 cm, corresponding to a slit length of $16.'7$ (See Fig. 11).

[‖]While the former enables a shorter exposure time for the alignment image (because the mirror is more efficient than a grating operating at 0-order), that time savings is negated by the several minutes required to change between a grating slider and the mirror slider. Since it only takes a few tens of seconds to tilt the grating to 0-order, that more than makes up for the longer exposure time.

Since no science data are acquired during the slitmask alignment process, the goal is to minimize the total amount of time required for that process. Because it can take the FCS one or more correction cycles to re-establish its servo lock on the FCS reference spectra (or reference spots if in direct imaging mode) after switching to a different instrument configuration, significant time savings could be achieved if FCS could be left in an idle state during slitmask alignment. Provided that FCS servo-lock is achieved in the spectroscopic configuration prior to switching to direct imaging mode for slitmask alignment, it has been demonstrated that FCS can be left idle during that alignment. Once slitmask alignment is completed and the instrument reconfigured for spectroscopic observations, the FCS automatically resumes its corrections using the FCS reference spectra obtained during the afternoon calibrations for that spectroscopic setting.

5. OPERATIONAL PERFORMANCE

Fig. 12 shows the flexure-induced image motion for one of the two sliders (slider 3) that hold the gratings (the results for the other grating slider are similar). This measurement was obtained by rotating DEIMOS continuously through 730° (i.e., from one rotation limit to the other) at a speed of 0.°05/second, first rotating in the forward direction and then rotating in reverse. While DEIMOS was rotating, images were obtained from the FCS CCDs about every 2° of rotation. The points obtained while rotating in the forward direction are connected by solid lines, while those obtained in the reverse direction are connected by dotted lines. The flexure pattern is not perfectly repeatable over each rotation, although there is more consistency between the curves for rotations in the same direction. A similar set of measurements was obtained, this time with FCS enabled, by rotating DEIMOS through 240° in the forward direction and at the same speed as in the previous measurement. Figs. 13 and 14 show the residual image motion with FCS enabled. (See poster paper for additional measurements.**)

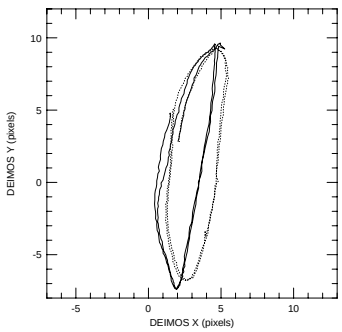

Figure 12. FCS disabled

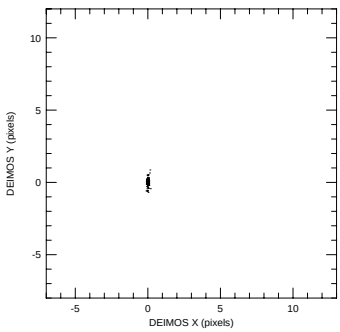

Figure 13. FCS enabled

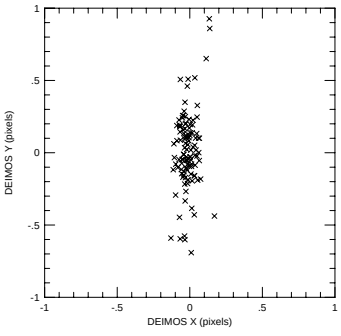

Figure 14. FCS enabled (detail)

6. CONCLUSION

The DEIMOS FCS has demonstrated that it is able to reduce image motion significantly and reliably, and thereby greatly improve the overall image quality and calibration accuracy of the data collected. The full implementation of the FCS software (including the FCS GUI) has significantly reduced the level of effort required to obtain FCS reference images during the afternoon and has resulted in an automated, turnkey system that operates with little need for observer intervention during nighttime observing. The DEIMOS FCS routinely performs at a level that meets its operational specifications and enables observers to achieve Poisson-limited sky subtraction.

ACKNOWLEDGMENTS

We thank Observing Assistants Gabrelle Saurage, Cynthia Wilburn, Ron Quick, and Joel Aycock of the W. M. Keck Observatory for their assistance with the commissioning of the DEIMOS FCS system. We also acknowledge the valuable feedback provided by Marc Davis, Alison Coil, Jeff Newman, Doug Finkbeiner, and other members of the DEEP Team during initial trials of the DEIMOS FCS software. We thank Elizabeth Chock, Jon Chock, Al Conrad, and Julia Simmons for their assistance in commissioning the overall software for the DEIMOS spectrograph. Thanks also to Vernon Wallace for assistance in generating the figures for this paper.

**http://www.ucolick.org/~kibrick/spie2004/deimos_poster_paper

DEIMOS was started in 1992 with a Facilities and Instrumentation grant from the National Science Foundation (ARI92-14621) in the amount of $1.79 million. The California Association for Research in Astronomy has so far contributed approximately $7.2 million directly to the project, not including the additional costs of CARA liaison and alterations that were needed for the Keck 2 telescope. UCO/Lick Observatory has contributed over $1 million so far in manpower.

REFERENCES

1. S. Faber *et al.*, "DEIMOS spectrograph for the Keck 2 telescope: integration and testing," in *Instrument Design and Performance for Optical/Infrared Ground-Based Telescope*, M. Iye, ed., *Proc. SPIE* **4841**, pp. 1657–1669, 2003.
2. R. Kibrick *et al.*, "A comparison of open versus closed loop flexure compensations for two Keck optical imaging spectrographs: ESI and DEIMOS," in *Instrument Design and Performance for Optical/Infrared Ground-Based Telescope*, M. Iye, ed., *Proc. SPIE* **4841**, pp. 1385–1398, 2003.
3. W. T. Deich, R. I. Kibrick, S. M. Faber, D. A. Clarke, and V. Wallace, "DEIMOS rotation control system software," in *Advanced Telescope and Instrumentation Control Software II*, H. Lewis, ed., *Proc. SPIE* **4848**, pp. 463–473, 2002.
4. R. Leach, F. Beale, and J. Eriksen, "New generation CCD controller requirements and an example: the San Diego State University generation II controller," in *Optical Astronomical Instrumentation*, S. D'Odorico, ed., *Proc. SPIE* **3355**, pp. 512–519, 1998.
5. C. Wright, R. Kibrick, and B. Alcott, "CCD imaging systems for DEIMOS," in *Instrument Design and Performance for Optical/Infrared Ground-Based Telescope*, M. Iye, ed., *Proc. SPIE* **4841**, pp. 214–229, 2003.
6. D. Clarke, "Dashboard: a knowledge-based real-time control panel," in *Proceedings of the 5th Annual Tcl/Tk Workshop*, pp. 9–18, 1997.
7. D. A. Clarke, S. L. Allen, G. D. Wirth, and A. C. Phillips, "Slitmasks from observer to telescope: astrometric slitmask manufacturing and control for Keck spectrographs," in *Advanced Software, Control, and Communication Systems for Astronomy*, H. Lewis, ed., *Proc. SPIE* **5496**, 2004.